Structure, Volume *28*

Supplemental Information

Mammalian Retromer Is an Adaptable Scaffold for Cargo Sorting from Endosomes

Amy K. Kendall, Boyang Xie, Peng Xu, Jue Wang, Rodger Burcham, Meredith N. Frazier, Elad Binshtein, Hui Wei, Todd R. Graham, Terunaga Nakagawa, and Lauren P. Jackson

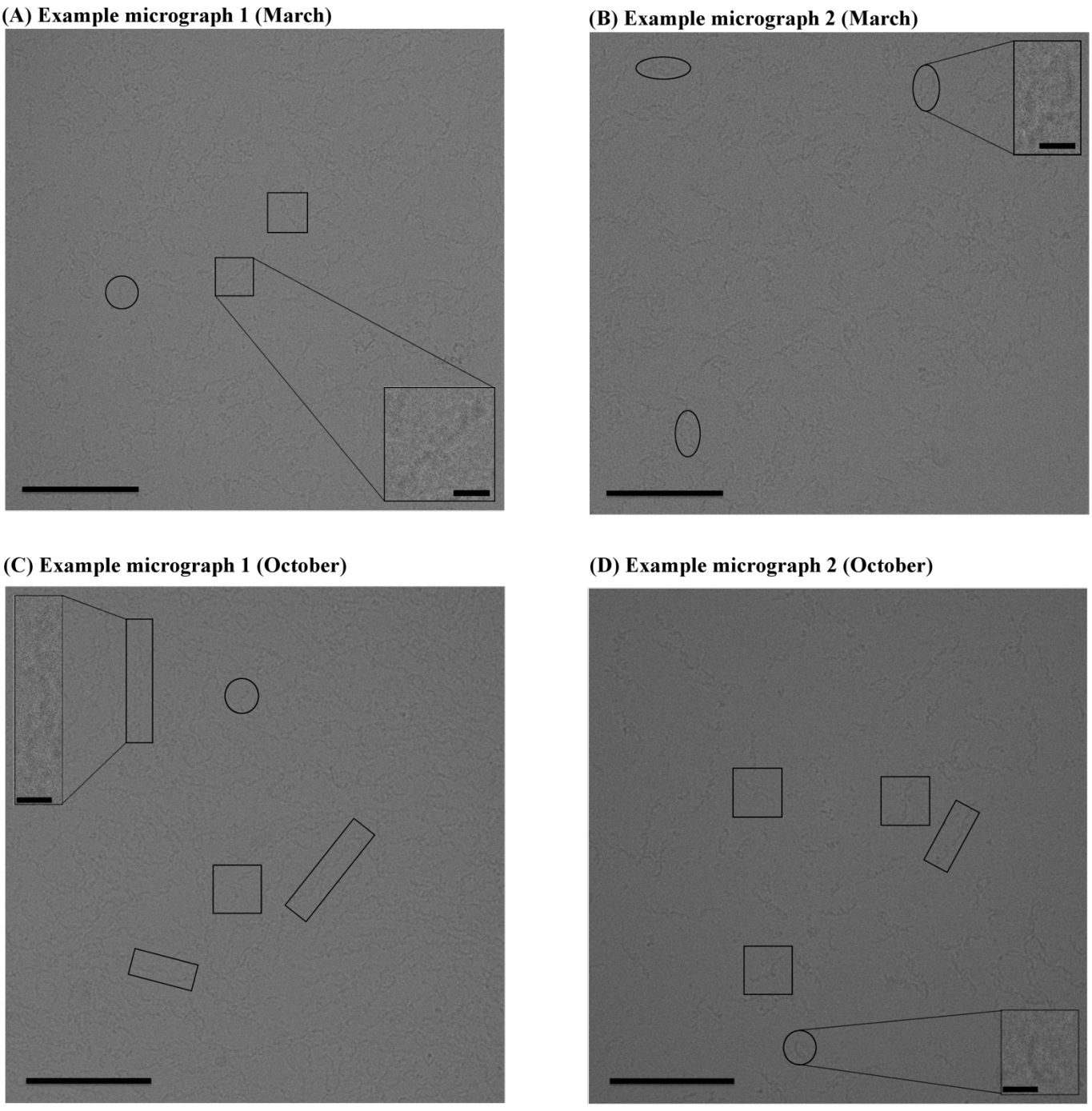

Figure S1. Retromer samples for cryo-electron microscopy, Related to Figure 1. Representative micrographs of retromer in vitrified ice. (A) and (B) show two micrographs from data collection #1 (March 2018). (C) and (D) show two micrographs from data collection #2 (October 2018). Heterotrimers are marked in circles; dimers are marked in squares; chains are marked in rectangles; and tetramers are marked in ovals. Scale bars represent 100 nm. Insets show close-up view of each particle type; scale bars for inset represent 10 nm.

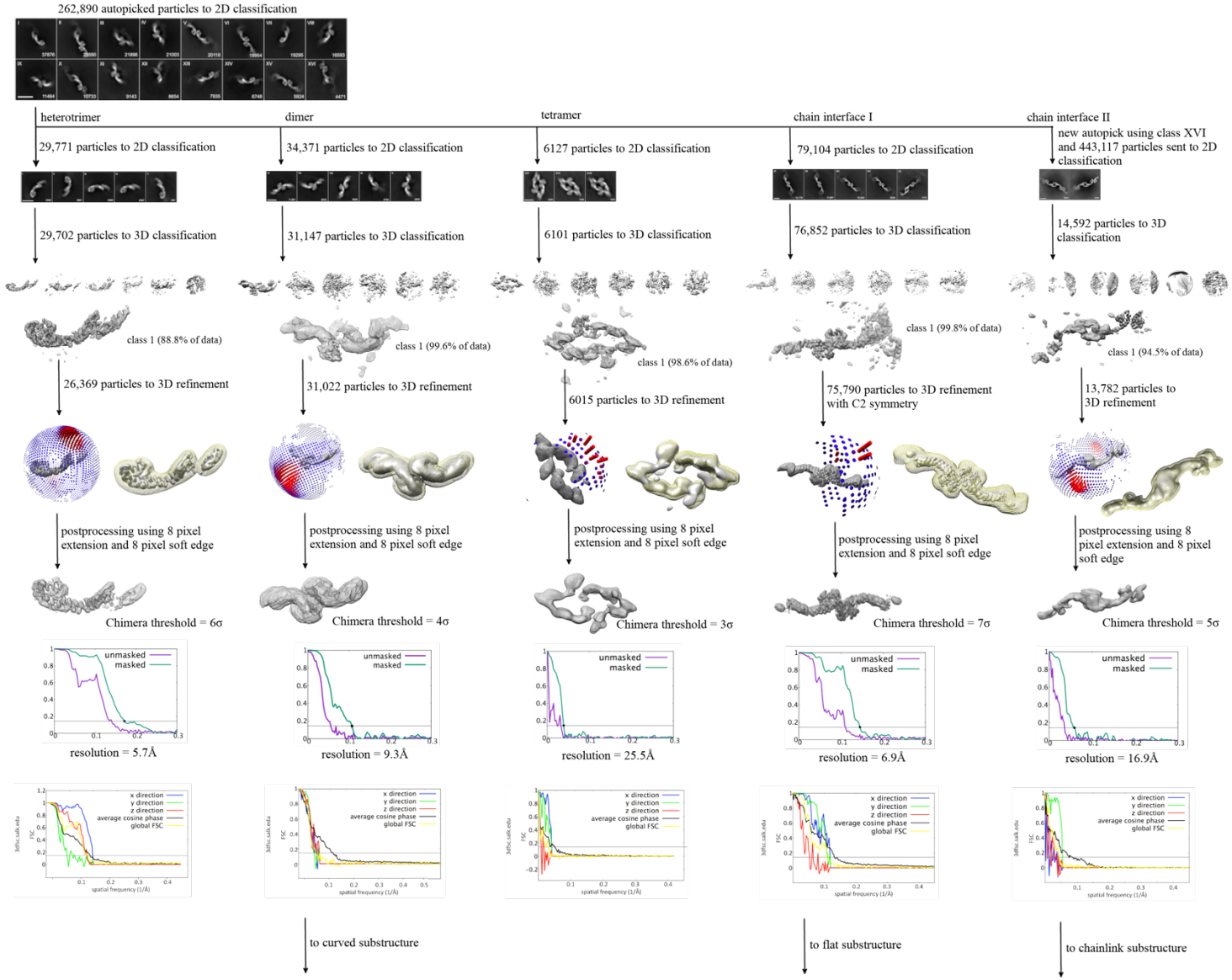

Figure S2. CryoEM image and data processing work flow, Related to Figure 1. The cryo-EM analysis workflow is shown. Particles were initially auto-picked from two combined datasets and then separated into 2D classes based on biochemical species (heterotrimer, dimers, two chain interfaces, and tetramers). 3D reconstructions were generated for each species. Fourier Shell Correlation (FSC) plots showing masked and unmasked resolution estimates from RELION are shown for each structure; grey dotted line marks the "gold standard" 0.143 cut-off, and the black dot marks masked resolution estimate reported in this figure, main text, and Table S2. The bottom row shows 3D FSC plots generated by the 3D FSC remote server.

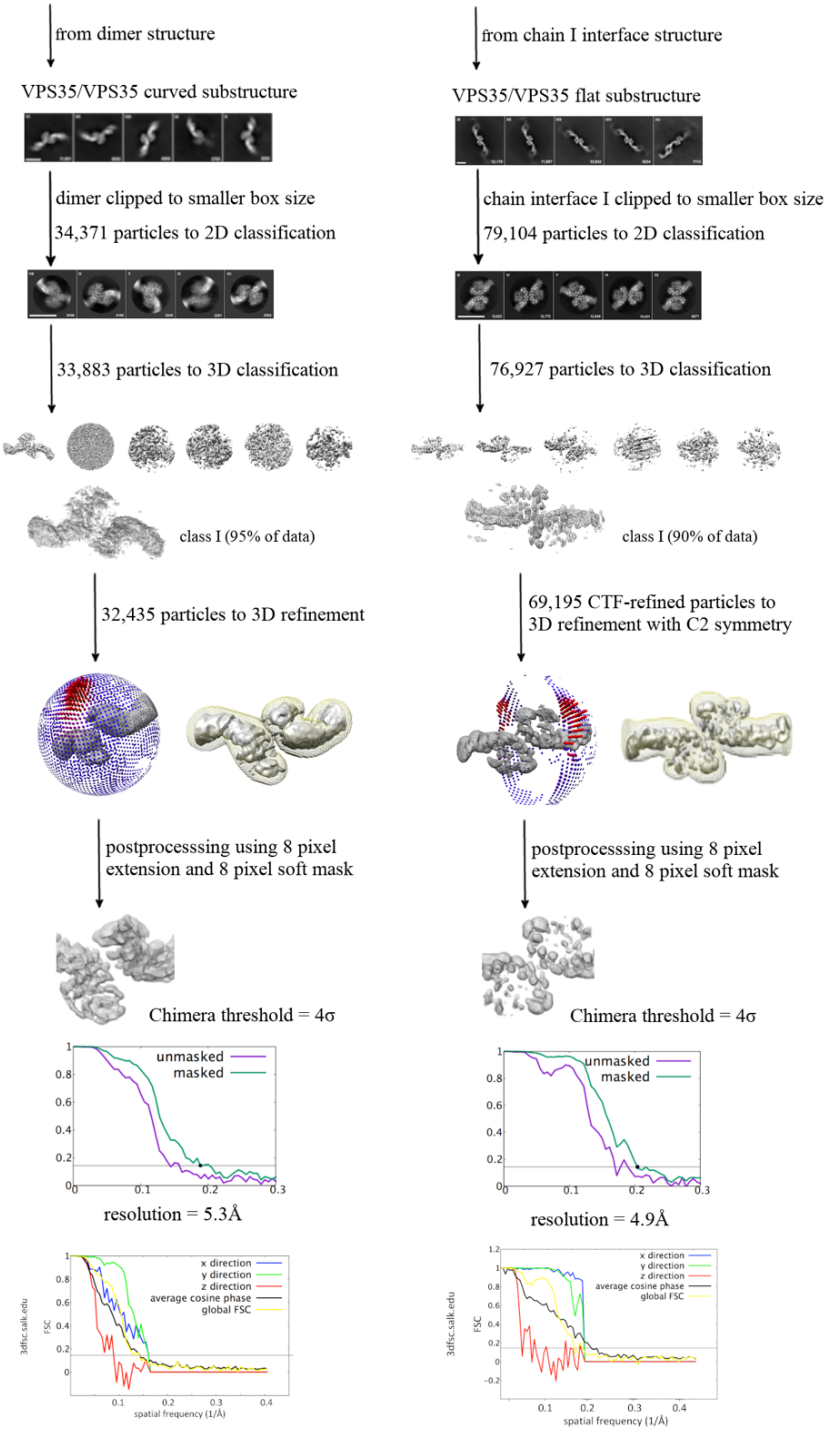

Figure S3. Cryo-EM data processing work flow for sub-structures, Related to Figure 4. The cryo-EM analysis workflow is shown for sub-structures determined from structures presented in Figures 1 and S2. The flat VPS35/VPS35 sub-structure was generated from chain interface I; the curved VPS35/VPS35 sub-structure from dimers; and the VPS26/VPS26 sub-structure from chain interface II. Fourier Shell Correlation (FSC) plots showing masked and unmasked resolution estimates from RELION are shown for each sub-structure; grey dotted line marks the "gold standard" 0.143 cut-off, and the black dot marks masked resolution estimate reported in this figure, main text, and Table S2. The bottom row shows 3D FSC plots generated by the 3D FSC remote server.

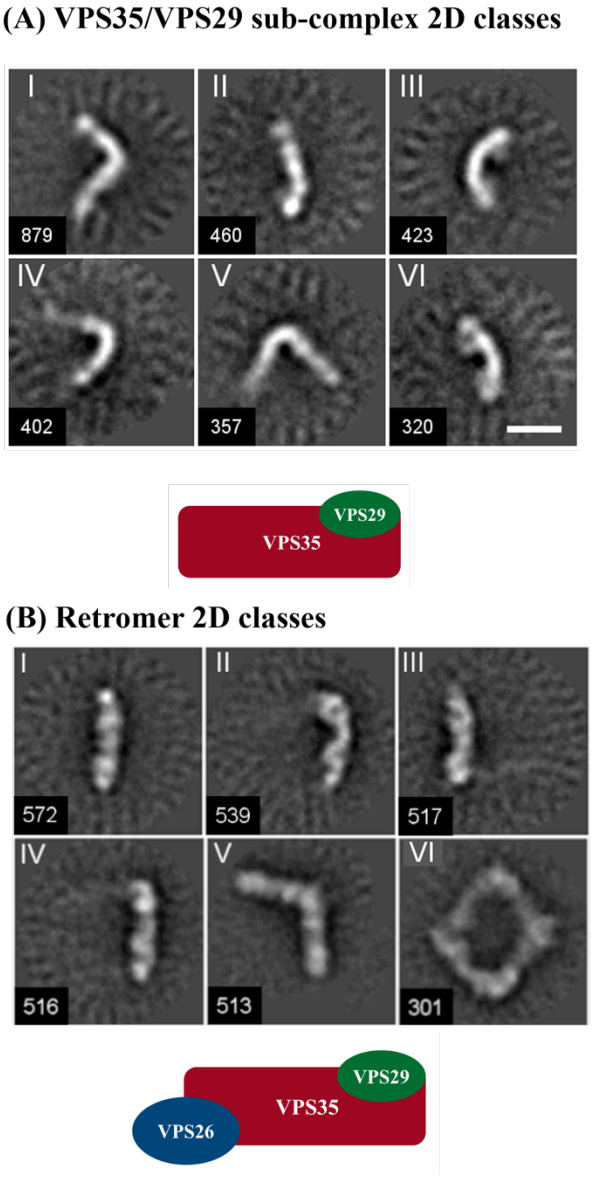

Figure S4. Retromer class averages in negative stain, Related to Figure 5. (A) Representative 2D class averages of negatively stained VPS35/VPS29 sub-complex particles. The VPS35/VPS29 sub-complex forms dimers but exhibits greater flexibility when VPS26 is absent. (B) Representative 2D class averages of negatively stained wild-type retromer. Scale bars represent 10 nm.

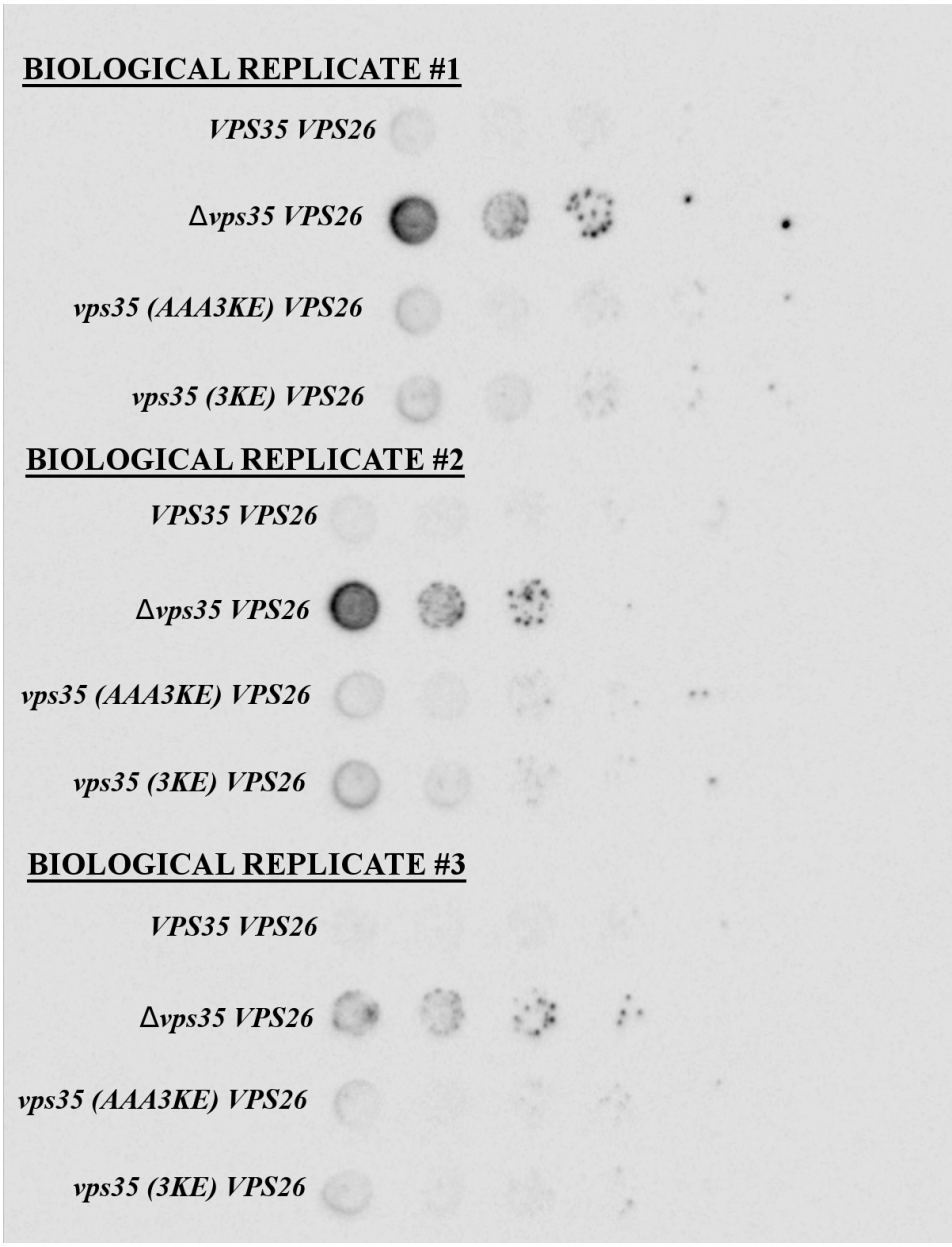

Figure S5. Carboxypeptidase Y (CPY) sorting assay in budding yeast, Related to Figure 6. Three biological replicates are shown from the CPY secretion assay. The box from replicate #1 represents the cropped blot shown in main Figure 4.

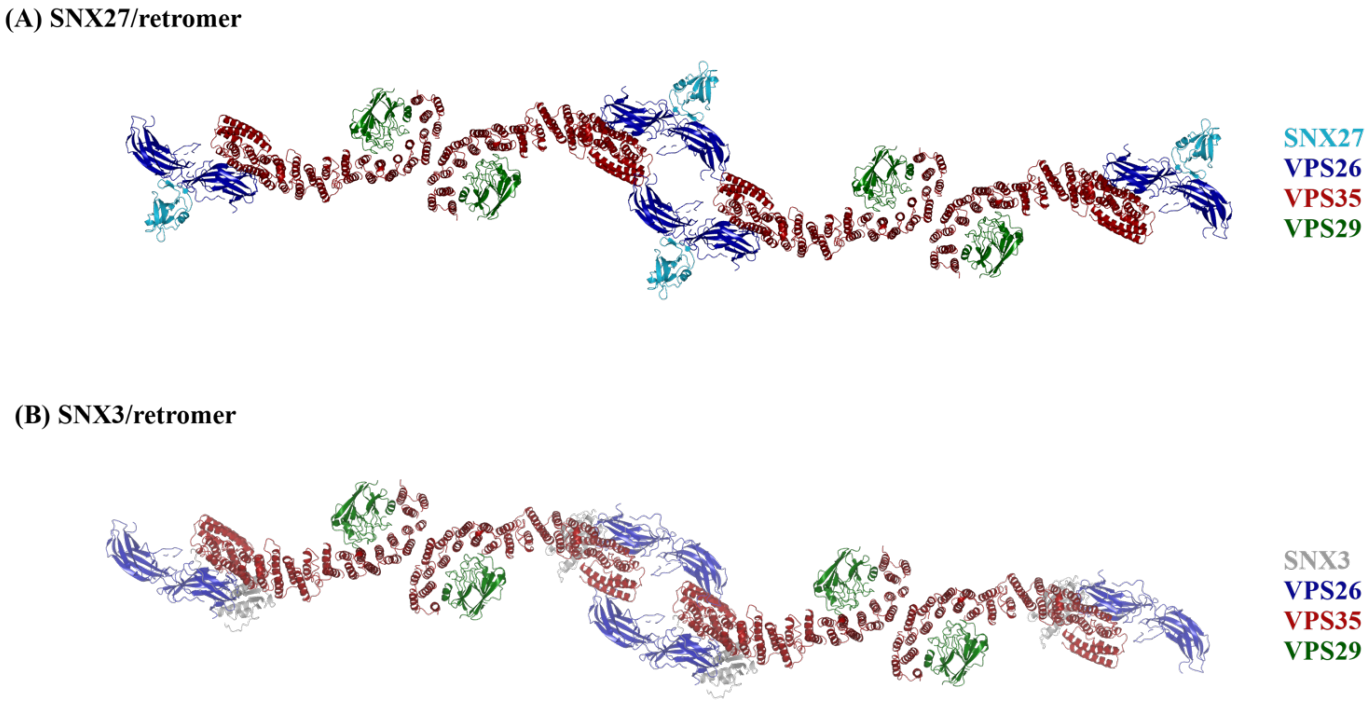

Figure S6. Models of flat retromer chains with mammalian sorting nexins, Related to Figure 7. (A) Top down view of SNX27/retromer chains with SNX27 PDZ domain shown in cyan; the PX and FERM domains are omitted. (B) Top down view of SNX3/retromer chains, with SNX3 PX domain shown in grey. VPS26 is shown in blue, VPS35 in red, and VPS29 in green.

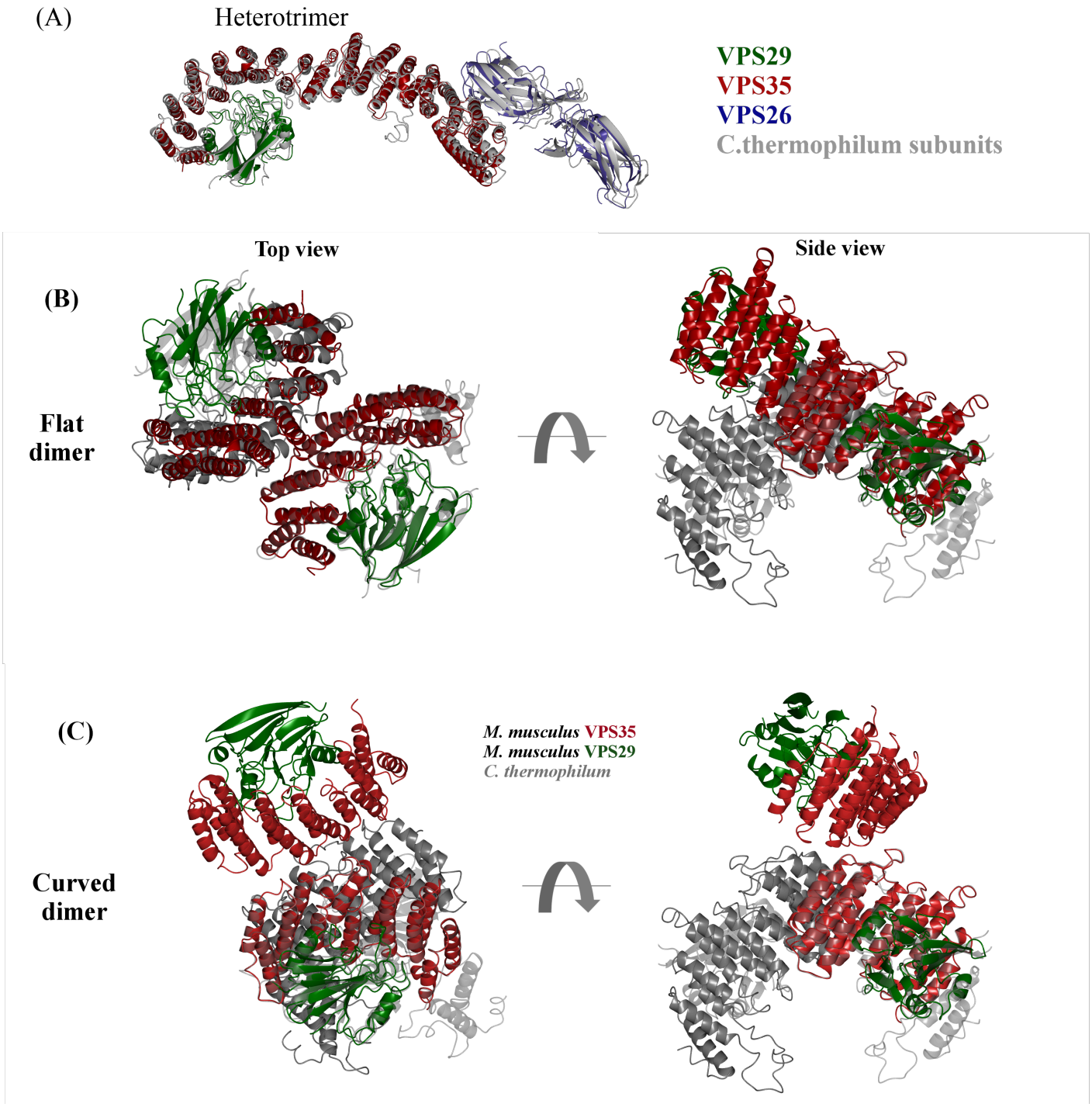

Figure S7. Comparison of mammalian and thermophilic yeast structures, Related to Figure 7. (A) Mammalian and thermophilic yeast structures determined from single particle cryo-EM and cryo-ET methods, respectively, are shown superposed in PHENIX (r.m.s.d. 1.1 Å). Mammalian subunits are shown by color with yeast subunits shown in grey. The flat (B) and curved (C) mammalian VPS35 dimers (VPS35 in red, VPS29 in green) were superposed onto the thermophilic yeast VPS35 dimer (grey) that forms the top of retromer arches when reconstituted on membranes with Vps5. Two views rotated by 90° are shown. Top views (left-hand column) are shown looking down onto the membrane from above. Side views (right-hand column) represents the apex of an arch.